

## 2 Preclinical Models of Tumor Growth and Response

*Patrick McConville, PhD, William L. Elliott, PhD, Alicia Kreger, BS, Richard Lister, BS, Jonathan B. Moody, PhD, Erin Trachet, BS, Frank Urban, MS, and W.R. Leopold, PhD*

### CONTENTS

INTRODUCTION  
TYPES OF TUMOR MODELS  
ENDPOINTS AND MEASUREMENTS  
SUMMARY AND FUTURE DIRECTIONS

### 1. INTRODUCTION

Experimental models of cancer have played an important role in cancer drug discovery for more than 60 years. The same models have proven critical as tools for the elucidation of the molecular basis of neoplastic transformation, the processes involved in tumor progression and metastasis, and the determinants of therapeutic success or failure. More recently, transgenic models in particular have been used to “validate” and prioritize new strategies for therapeutic intervention. *In vivo* cancer models can be considered to fall within two broad classes, transplantable models, and *in situ* models, each with a number of subtypes (Fig. 1). For pragmatic reasons, transplantable models as a group are the most commonly used for drug evaluation, while *in situ* models such as cancer-prone transgenic mice provide a rich source of information on cancer etiology. It should be noted that each transplantable model represents the tumor of a single patient, not a tumor type. This discussion is centered on the application of both model types, and the potential impact of imaging technologies for cancer drug discovery. However, with recent advances in preclinical imaging technologies, these models are also proving useful in the development and testing of new imaging techniques and contrast agents. Increasingly, with the expanding role of drugs tied to specific molecular

From: *Cancer Drug Discovery and Development*  
*In Vivo Imaging of Cancer Therapy*  
Edited by: A.F. Shields and P. Price © Humana Press Inc., Totowa, NJ

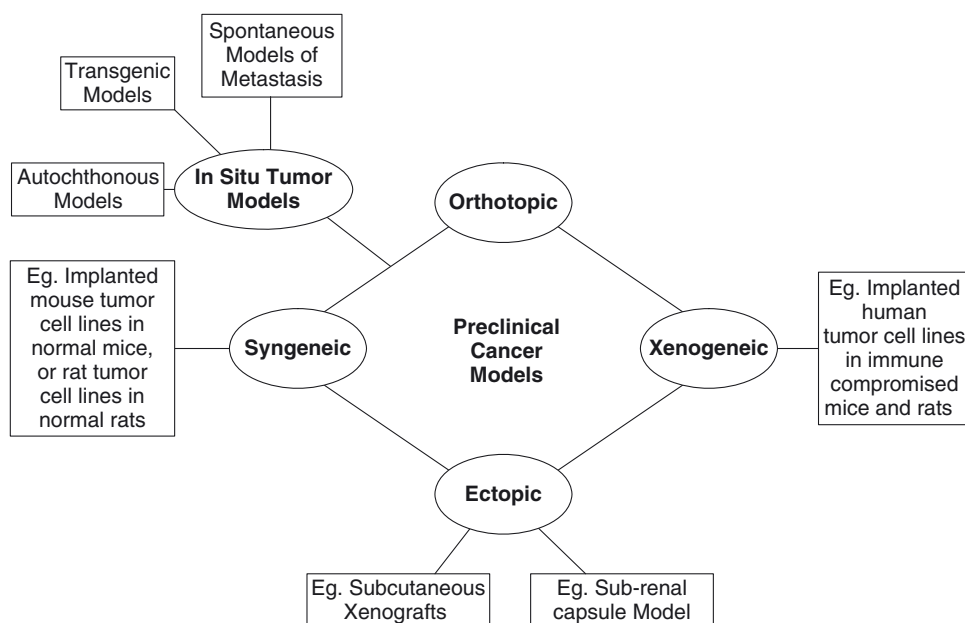


**Fig. 1.** Schematic representation of the broad categories of preclinical cancer models in use today. *In situ* tumor models can be subcategorized by the method for induction of the tumor. Transplantable tumor models are commonly subcategorized according to whether the tumor is implanted in the organ in which the cell line originated (orthotopic versus ectopic) and in the species in which it originated (syngeneic versus xenogeneic).

targets, these models are also being used to optimize and validate clinical imaging strategies. Finally, molecular imaging techniques are finding a critical role preclinically in the simultaneous confirmation of mechanism of action and assessment of efficacy. This is particularly true in orthotopic or transgenic model systems.

## 2. TYPES OF TUMOR MODELS

### 2.1 Transplantable Syngeneic Models

Transplantable syngeneic leukemia and solid tumor models were developed from spontaneous or induced tumors subsequently adapted to serial *in vivo* passage in the same animal strain. The majority of early syngeneic models were leukemias, the most familiar of which are P388 and L1210 (1–4). Syngeneic transplantable solid tumor models were developed in the 1960s and 1970s by exposure of rodents to chemical carcinogens. This provided a variety of tumor histotypes and tumors with different growth rates within each histotype (5–11). Development of these tumor models was pioneered by investigators such as Fidler (12, 13), Morris (5, 14), Skipper (15–17), Schabel (18–20), Griswold (21–23), and Corbett (7, 8, 24–26).

Early drug screening strategies often involved an initial experiment against a murine leukemia with life span as the measured endpoint (27). Active compounds typically then moved into a solid tumor screening panel (15, 16, 18, 19, 28, 29) wherein solid tumor fragments were implanted into the subcutaneous space, and therapy was assessed by caliper measurement (27). Advantages of these models include their low cost and reproducibility. Imaging was generally not needed for assessment of tumor response in

these easily accessible and observable tumors. However, many investigators have used such models in the development and testing of new imaging approaches. In addition, the tumors grow in an immune-competent host, making these models appropriate for the study of immune modulation and vaccine approaches. However, the genetics of murine cancer are not always identical to their human counterparts, reducing the expectation of a direct correlation with clinical experience. The lack of progress in treatment of the major human solid tumors led to the conclusion that screening strategies with leukemias as the first triage point may not be appropriate (30). Subsequently, many investigators adopted screening strategies that involved direct testing against a panel of solid tumors.

## ***2.2 Spontaneous and Autochthonous Models***

There has been a resurgence in autochthonous models (31–33), such as mammary (34) and colon tumors (35) induced in rats with a carcinogen. The major theoretical advantage of both spontaneous and autochthonous models is that they may be more relevant to the development of human disease because the tumors reside in the tissue appropriate for the histotype. However, studies against tumors induced in this fashion are difficult because of low tumor incidence, variable and delayed onset of tumor growth, and deep tissue location of the tumors. Often treatment is initiated on an animal-by-animal basis as tumors arise and assessment of tumor burdens is performed by terminal sacrifice, complicating treatment and data collection. Lastly, autochthonous model systems require the handling and administration of known potent human carcinogens.

## ***2.3 Human Tumor Xenografts***

Syngeneic models, however well characterized, are not human. Xenotransplantation is the transplantation of tissues or organs from one species into a different species. The application of xenotransplantation techniques to the growth of human tumors in experimental animals was a major breakthrough in cancer biology and drug discovery research.

### **2.3.1 SUBRENAL CAPSULE**

One of the first of these models sought to take advantage of the immunologically privileged status of the subrenal capsule (SRC) (36, 37). Human tumor fragments implanted under the SRC are not subject to immediate rejection. Changes in tumor volume during therapy are determined by invasive measurements with an ocular micrometer. Unfortunately, the SRC xenograft assay is labor intensive and both tumor growth and response to therapy are often highly variable.

### **2.3.2 HUMAN TUMOR XENOGRAFTS IN IMMUNODEFICIENT ANIMALS**

A major breakthrough in the *in vivo* evaluation of novel agents against human tumors was the identification and characterization of immunodeficient mice and rats. These animals have genetic immune deficiencies that minimize or prevent the rejection of the grafted tissues from other species. The difficulty in using immune compromised animals is that they are highly susceptible to viral, bacterial, and fungal infections. These infections can alter the outcome and reproducibility of experiments. Therefore, immunodeficient animals are maintained in specific pathogen-free (SPF) environments, dramatically increasing research costs (38, 39).

*Nude*, *scid*, *xid*, and *beige* mice are the four primary types of immune-deficient mice. Each type of immunodeficient mouse has one or more mutations that diminish the animal's capacity to reject transplanted allografts and xenografts. None of the mutations completely eliminates the immune system function (40–50). *Nude* and *scid* mice are predominantly used for cancer drug evaluation. Xenografted tumors often exhibit a more neoplastic phenotype in *scid* mice than in nudes, presumably because of the more severe immune deficiency of *scid* mice. These animals are often crossed with *beige* and/or *xid* mice to further suppress immune function. The availability of these animals transformed drug discovery paradigms. However, the costs of purchasing and maintenance of these animals is many fold higher than that of conventional animals.

### 2.3.3 METHODS FOR XENOGRRAFT STUDIES IN IMMUNODEFICIENT MICE

**2.3.3.1 Subcutaneous Xenografts.** Subcutaneous xenografts are human tumor xenografts (cells, brei, or fragments) that are injected underneath an immune-deficient animal's skin and not into the underlying tissue or cavities. These models are cost effective, and provide a direct assessment of efficacy against a human cancer through simple, noninvasive caliper measurement of tumor size. The accessibility of the tumor is also an advantage for harvesting of tumor tissue. Several publications have suggested that human tumor xenograft models are better predictors of clinical activity than syngeneic models (51–55). Although the use of human tumor xenografts has many advantages, there are also a number of disadvantages. Human cells are placed in a murine environment creating interactions that may not faithfully reflect the human disease process (e.g., differences in the local cellular environment, cytokine, chemokine, and growth factor incompatibility, differences in immunologic state, etc.). Moreover, the subcutaneous environment of the xenograft may also fail to recapitulate normal interaction of the tumor and stroma. Other disadvantages of this model include occasional tissue ulcerations, loss of metastatic potential, and dedifferentiation of the tumor. In addition, the genomic instability of human cancer requires that considerable care be taken to avoid unintended change of the model over time and multiple passages. Despite these potential shortcomings, human tumor xenograft testing remains the mainstay of *in vivo* anticancer therapeutics evaluation.

**2.3.3.2 The Hollow Fiber Assay.** The hollow fiber assay (56) utilizes polyvinylidene fluoride hollow fibers inoculated with human tumor cell lines (57). The fibers are then sealed and implanted into the intraperitoneal cavity or subcutaneous space of an immunodeficient mouse for 3–10 days. After treatment, the fibers are removed and live cells are counted. Advantages of this method are that multiple cell lines can be tested simultaneously in one animal contributing to low cost and high throughput. Disadvantages are that the technique requires survival surgery, the tumor cells are unable to interact with the normal stroma, and the cells have no opportunity to develop a blood supply. Hence, this assay does not reflect treatment-induced changes in stroma-tumor interactions and vascular effects.

## 2.4 Orthotopic Models

An orthotopic model involves the implantation of a tumor into the organ from which it arose. This is an increasingly popular assay format. A theoretical advantage of this

format is that the tumor cells grow in the “context” of their native *in situ* environment (58–60). Orthotopic models have additional advantages over subcutaneous and hollow fiber systems besides cell context. These advantages may include retention of differentiated structures within the tumor, vascular growth differences, more realistic tissue pharmacokinetics at the tumor site, and metastatic spread. However, tumor implantation for orthotopic models requires potentially complex survival surgery. Observation of tumor growth in internal organs typically requires serial sacrifice of cohorts of animals, tumor take rates and growth can be highly variable, and it may be difficult and costly to harvest tumor tissue for pharmacodynamic and pathological analyses. These factors increase cost and decrease throughput. The use of imaging technologies can dramatically enhance the efficiency of orthotopic models. Although it is generally accepted that orthotopic implants often better preserve various aspects of tumor biology, demonstrations that they give different or more predictive assessments of therapeutic potential are lacking. The recent focus on signal transduction pathways (where context may be important) as targets for cancer drug discovery has renewed interest in the relevance of this assay format.

### 2.5 Models of Metastasis

While the general stability of the tumor tissue in the models discussed above can be an advantage, they often lack key features of human cancer, such as metastasis to secondary organ sites. Prevention of the metastatic process and specific targeting of metastatic lesions offers opportunities for therapeutic intervention. However, reproducible animal models of metastasis that recapitulate all aspects of the metastatic cascade are rare.

Clinically, metastases to the lungs, regional lymph nodes, liver, and brain are most common. A major determinant of the metastatic site is simply location of the primary tumor and the next capillary bed capable of trapping blood-borne tumor emboli. However, the process of metastasis is also critically dependent on the ability of cells that metastasize to promote angiogenesis and proliferate in the new organ environment, giving rise to the “seed and soil” hypothesis (61–64).

Several models of metastasis employ direct or systemic injection techniques. The choice of the site or route of injection is generally based on vascular proximity to the target organ. For example, liver metastases models often rely on intrasplenic injection, lung metastases can be reproducibly obtained from tail vein injection, and bone metastases from intracardiac injection. While direct injection models generally provide the most reproducible and cost-effective models, they have the limitation of not encompassing the entire metastatic process.

Spontaneous models of metastasis, including subcutaneous, transgenic, orthotopic, and autochthonous models provide a better representation of the entire metastatic process than direct injection models, and are specifically suited to the testing of therapeutics for prevention of metastasis. The most common of these relies on continuous passage of metastatic lesions arising from subcutaneous tumors to maintain target organ specificity and metastatic potential. However, these models require longer staging periods and generally have poorer reproducibility and organ specificity than direct injection methods. In addition, these models may require excision of the primary tumor.

Regardless of the model, the study of metastatic lesions has traditionally required inefficient experimental designs that involve serial sacrifice of cohorts of animals. However, *in vivo* imaging technologies can dramatically facilitate these assessments and are finding increased use.

## 2.6 Transgenic Tumor Models

The massive shift of drug discovery efforts toward inhibition of specific oncogene or suppressor gene related targets has led to increased interest in the use of transgenic models for target validation and the evaluation of drug candidates (65–70). Transgenic tumor models are created by the introduction of heritable (germ line) or somatic mutations that are implicated in neoplastic transformation. Target genes can be replaced by new alleles, conditionally expressed, conditionally turned off, or mutated. A key advantage of transgenic models is that the etiology of tumor development closely mimics that in humans. The animals can be treated with therapeutic agents at any stage of tumor development to further elucidate therapeutic efficacy and the mechanism of action (71).

Three examples of transgenic mouse models with germline mutations are the TRAMP (transgenic adenocarcinoma of the mouse prostate) model, and the p53 and PTEN knockout mice. The TRAMP model was created by linking the prostate-specific pro-basin promoter to the SV40 large T antigen. These animals develop variably differentiated tumors that metastasize primarily to the lungs and lymph nodes (71, 72). This model has been used to study late events in prostate tumorigenesis and mechanisms of angiogenesis. p53 is the most commonly mutated gene in human cancer. In the p53 knockout mouse, the p53 tumor suppressor gene is inactivated by mutation to create a model of the human Li-Fraumeni familial cancer predisposition syndrome. These mice are more susceptible to spontaneous and carcinogen-induced tumors in many organs (70). The average tumor latency for a homozygous p53 (–/–) mouse is about 4.5 months with an increased latency period for heterozygous p53 (–/+) animals (73). The PTEN heterozygous knockout mouse is predisposed to many tumor types, including colon carcinomas, leukemia, germline tumors, and T cell lymphomas (71, 74). Elimination of one PTEN allele results in the inactivation of proapoptotic pathways possibly contributing to drug resistance. The PTEN double null (–/–) is an embryonic lethal mutation.

Transgenic models driven by germline mutations can be problematic. Mutations of interest are often embryonic lethal. Additionally, unwanted physiological or toxic effects during development may occur that render the model unusable. Organ specificity can also be difficult to control and the study of multiple gene defects can require complex breeding efforts. Lastly, these animal models are often characterized by long tumor latency periods.

Somatic cell modification strategies offer advantages over germline modification strategies that include improved tissue specificity of transgene expression, avoidance of embryonic lethal events, and opportunities for introduction of sequential multigene defects. An example of a transgenic mouse model created by somatic cell mutation strategies is the TVA model, which is based on retroviral gene transfer. A transgenic animal is created that expresses the avian leukosis virus (ALV) receptor 1 (TVA) from a tissue-specific promoter. These animals are not predisposed to develop cancer without further manipulation. The target gene construct of interest is cloned into a replication-



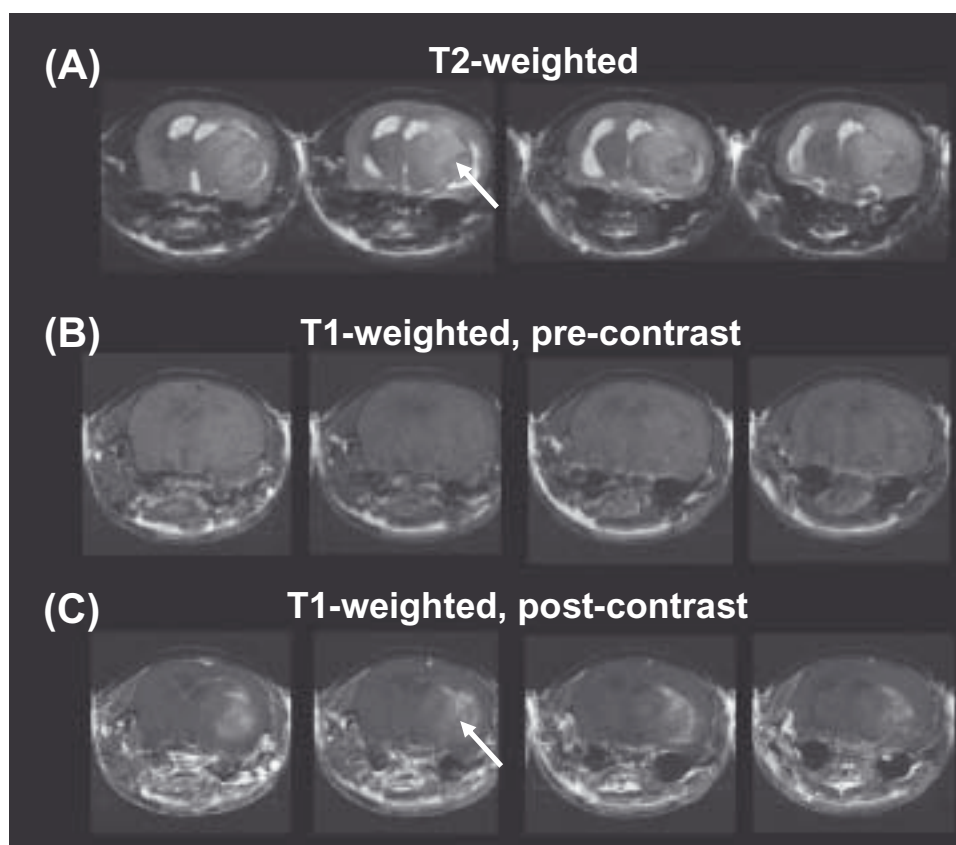


**Fig. 2.** MRI of PDGF-induced glioma in a Ntv-a mouse (76). The same four contiguous slices are shown for (A) T2-weighted scans showing the tumor as a hyperintense region in the right upper cortex, and T1-weighted scans (B) before, and (C) after administration of Gd-DTPA. The T1-weighted scans highlight localized, heterogeneous contrast enhancement in the tumor. The MRI appearance of glioma in this model is typical of that of human glioma.

competent ALV splice-acceptor (RCAS) vector followed by direct injection of the modified virus or virus-infected cells into the TVA-expressing tissue (75). The TVA/RCAS system has been used in mouse models of induction of gliomas (76) (Fig. 2) and ovarian cancer (77, 78).

### 3. ENDPOINTS AND MEASUREMENTS

Diverse types of information may be gleaned from any of the tumor models described above. Historically, with the exception of transgenic systems, these models have been used primarily to simultaneously assess the response of tumors to drug treatment and the potential for host toxicity (therapeutic index). Imaging technologies are routinely used for anatomical detection of tumors, particularly in orthotopic, metastatic, and transgenic models. However, trends toward molecular-targeted therapies are increasing the use of imaging technologies for quantifying drug-induced changes in physiology. Such methods can enable the use of endpoints that are tied to target modulation, in addition to more traditional growth-based endpoints.

### 3.1 Detection or Diagnosis of Tumors

The basic method of tumor detection and quantitation is visual observation. Traditionally this involves palpation followed by caliper measurements. Calculation of tumor volume and an assumption of unit density generate an estimate of tumor burden. Caliper measurements have proven representative when compared to actual weights of excised tumors. This detection method is cost effective but primarily limited to subcutaneous tumors.

Increased interest in orthotopic and transgenic systems has created a demand for imaging-based methods for tumor diagnosis or detection. A broad array of imaging modalities and techniques is available for *in vivo* detection of tumors in mouse cancer models. These include bioluminescence imaging (BLI) and *in vivo* fluorescence imaging, magnetic resonance imaging (MRI), magnetic resonance spectroscopy imaging (MRSI), X-ray computed tomography (CT), positron emission tomography (PET), and single photon emission computed tomography (SPECT). Additional technologies not discussed in this chapter include ultrasound imaging and optical coherence tomography.

*Bioluminescence imaging and fluorescence imaging—in vivo:* BLI is a recently developed optical imaging method that allows visualization of luciferase-driven light emitted from within an animal (79, 80). In the most basic application, mice are inoculated with tumor cells that have been stably transfected with the luciferase gene, and the constitutive expression of luciferase allows assessment of tumor burden after systemic injection of substrate (luciferin). High sensitivity and the ability to quantify tumor burden make BLI ideally suited to detection of the spread and growth of metastases and *in situ* tumor models. Throughput is also high since image acquisition is generally rapid and several mice may be imaged simultaneously. Low spatial resolution is a limitation of BLI. In addition, since the images are commonly two dimensional, images from several animal positions may be necessary to unambiguously identify the anatomical location of a given signal.

*In vivo* fluorescence imaging can also be used to detect and monitor tumor growth in small animals (81–83). The fluorescent signal is emitted following excitation with monochromatic light of fluorescent proteins or dye-labeled biological molecules. Unlike BLI, fluorescence imaging does not require the injection of exogenous substrate. In addition, the high fluorescence signal allows image acquisition on a millisecond time scale, compared to minutes for BLI. Signal attenuation in deep tissues and a high background of autofluorescence can be problematic for standard fluorescent compounds, however, newer imaging agents provide fluorescent emission at the near-infrared wavelengths that minimizes these effects (84).

*Magnetic resonance imaging:* MRI of preclinical tumor models combines outstanding soft tissue contrast with high spatial resolution (85–87). Due to differential MR relaxation properties, tumors can usually be distinguished from normal tissue in rapid anatomical scans (Fig. 2). Another common approach to detection of tumors is with a contrast agent such as gadolinium diethylenetriaminepentaacetic acid (Gd-DTPA). Differential uptake of the contrast agent by the tumor compared with surrounding normal tissue, allows the tumor to be delineated in MR images (Fig. 2). MRI has been used in mouse models to detect tumors in the brain, lung, liver, and pancreas, among others (87). Tumors as small as 0.5 mm in diameter can be detected and monitored *in vivo* using MRI.



*Magnetic resonance spectroscopic imaging:* MRSI involves the combination of MR imaging techniques with conventional NMR spectroscopic methods (commonly proton or phosphorus based) to provide spatially localized spectra. Pathological tumor biology provides unique spectral signatures of various metabolites that distinguish tumors from normal tissue. For example, metabolites such as choline, creatine, lactate, ATP, lipid, and lysine can differentiate certain tumor types from surrounding normal tissue, as well as distinguish between benign and malignant disease in some cases (85, 88).

*Computed tomography:* The application of high-resolution X-ray CT to preclinical cancer models has recently become feasible, particularly for detection of lesions in bone, lung, and mammary glands (89). Three-dimensional images with resolution on the order of a 10–50  $\mu\text{m}$  are produced. With the use of CT contrast agents and blood pool agents, soft tissues such as liver, pancreas, spleen, and kidney, as well as vasculature can also be imaged (89).

*Positron emission tomography:* PET is increasingly used to study tumor biology. Equipment design and sensitivity have improved, allowing higher image resolution and animal throughput. Tumor detection using micro-PET takes advantage of pathological changes in tumor cells that promote enhanced uptake of positron-emitting radiotracers. PET tracers have been developed to measure cellular glucose metabolism ( $[^{18}\text{F}]$ fluoro deoxyglucose, FDG), cellular proliferation ( $[^{18}\text{F}]$ fluorothymidine, FLT), protein synthesis ( $[^{11}\text{C}]$ methionine, MET;  $[^{18}\text{F}]$ tyrosine), as well as transgene expression (90–96). An alternative method  $[^{124}\text{I}]$  uses radioimmunotracers targeting tumor-specific antigens that provides distinction between normal and malignant tissues (97, 98).

### 3.2 Assessments of Change in Tumor Burden

Change in tumor burden, usually in response to drug treatment, has historically been measured directly with calipers, by weight of an excised tumor mass, or by inference from measurement of host lifespan (1, 27). Excised tumor masses and tumors measured *in situ* contain both viable and dead tissue, and gross assessment of their mass is not equivalent to determination of the surviving fraction. The surviving fraction can be estimated for excised tumor masses by *in vitro* determination of clonogenic survival (99).

By far the most common format for the determination of therapeutic effect involves the estimation of tumor burden from caliper measurements of subcutaneous tumor masses. A number of mathematical treatments of these types of data have been developed, but two are dominant. The most common assesses response to therapy by comparison of control and treated tumor burdens as simple ratios of tumor mass ( $T/C$ ) at a single point in time. Alternatively, ratios of the change in mass over the course of treatment ( $\Delta T/\Delta C$ ) are generated (100, 101). This method is quick and economical, but it is also prone to severe variability, and the results are not directly comparable between experiments or across models. In addition, the same data set can give different estimates of therapeutic effect depending on the day of measurement, making the data highly subjective. Finally this method cannot give a quantitative estimate of the number of tumor cells surviving treatment. An alternative approach, pioneered by the group at Southern Research Institute, uses more data points to assess a therapy-induced tumor growth delay ( $T-C$ ) from which estimates of net change in tumor burden are derived

(27). The advantages of this more rigorous method are that it produces data that are *quantitatively* comparable between experiments and across models.

As the use of transgenic, orthotopic, and metastasis models increases, all of the imaging modalities described above are being increasingly utilized for detection of tumor masses and measurement of the effect of therapeutic intervention. Imaging can greatly increase the efficiency of these models and provide a more accurate assessment of tumor burden than traditional determination after serial sacrifice. However, imaging can be associated with increased cost and decreased throughput. In certain cases, the use of a contrast agent or labeled molecule may also be required for image-based assessment of tumor burden, which may further increase the complexity of the assay.

### 3.3 Pharmacokinetics

Pharmacokinetic analysis quantifies the processes of absorption, distribution, metabolism, and elimination (ADME) of compounds over time. Often this is accomplished through serial collection and analysis of body fluids or tissues, or by autoradiography to generate a concentration–time profile. These traditional methods typically consume large numbers of animals, time, and resources.

In autoradiography, animals are systemically exposed to radiolabeled compounds and sacrificed at specific time points. Frozen tissue sections are exposed to imaging plates to produce high-resolution images directly from tissue samples (102). Two-dimensional images can then be stacked to form a three-dimensional image (103). However, this technology is time and labor intensive and relies on the use of potentially hazardous and long-lived radioisotopes.

As imaging modalities have advanced, a number of techniques have been applied to the determination of pharmacokinetic profiles. Positron emission tomography and SPECT have shown particular promise in this respect. These imaging technologies can be used to track movement of compounds, formation of metabolites, tissue concentrations, and drug half-lives. These are noninvasive imaging modalities that image radio-tracer distribution after systemic injection into the animal. However, quantification can be problematic due to tissue scattering of emitted photons. While PET is 10- to 20-fold more sensitive with better image resolution than SPECT (104), the generally shorter half-lives of PET isotopes can make the generation and use of labeled compounds challenging. Both imaging modalities are broadly applicable in clinical and preclinical settings.

### 3.4 Drug Effects at the Molecular Target

The dramatic shift of cancer drug discovery efforts toward a focus on specific molecular targets over the past decade has prompted an increased interest in pharmacodynamic analysis of drug function. These analyses confirm target modulation and can allow quantitative correlation of target modulation with both pharmacokinetics and preclinical efficacy (105–107). Pharmacodynamic analyses can also be used productively to enhance the efficiency of the discovery process by preempting doomed efficacy determinations. Pharmacodynamic analyses to determine the extent and duration of target modulation are typically rapid (1–2 days), and they require minimal drug supplies and only a few animals. By comparison to efficacy testing against a xenograft model, a pharmacodynamic analysis consumes 10- to 25-fold fewer resources. It can allow

efficient “drop” decisions for weak compounds and enable an informed design (with respect to dose selection and treatment schedule) of efficacy experiments for compounds with strong potential. Optimization of *in vivo* function for target modulation prior to efficacy determination is becoming the discovery paradigm of choice for targeted programs. These correlations can also be used to set decision-making thresholds for biomarker analyses in phase I clinical trials. Failure to reach a predetermined threshold for target modulation at tolerated dose levels would prompt a decision to terminate development of the targeted compound.

Pharmacodynamic analysis traditionally has involved harvest of tumor tissue from treated animals and quantitative assessment of target modulation with techniques that include Western or Northern blot analysis, biochemical assays for enzyme activity, or immunohistochemistry. More recently *in vivo* imaging-based assays have been developed to measure changes in enzyme activity, substrate or reaction product concentrations, and protein interactions. Imaging-based pharmacodynamic analyses using modalities such as bioluminescence, fluorescence, PET, and SPECT are becoming more widely used. They offer simultaneous evaluation of drug function at the molecular level and efficacy at the whole animal level, dramatically increasing efficiency, reducing animal use, and generating tighter correlations.

Extensions of the basic BLI experiment include various strategies for coupling the expression or activation of luciferase to molecular events within the cell, so that the event is signaled by light production of the active luciferase (79, 108). For example, BLI has been used to image DNA damage *in vivo* with a transgenic mouse that harbors an Mdm2-Luc cassette. Events that induce DNA damage cause stabilization of p53 wherein it accumulates approximately 100-fold, followed by induction of p53 transcriptional activity, leading to activation of the Mdm2 promoter. Subsequent luciferase expression can be detected by BLI. This has been used to demonstrate the radio-sensitizing effect of 5-fluorouracil in mice (A Rehemtulla *et al.*, University of Michigan, 2003, personal communication).

### 3.5 Drug-Induced Physiological Changes

Direct assessment of drug function at the molecular target is often difficult or impossible. This is particularly true in the clinic, where the requisite biopsies may not be possible. In these situations, surrogate or indirect measures of drug-induced changes in physiology can be useful. Perhaps the best examples are assessments of drug-induced changes in tumor blood flow, vascular density, and vascular permeability now popularly applied to the development of antiangiogenic agents (109–111). However, a key difference between most clinical and preclinical imaging applications is the preclinical use of anesthesia such as isoflurane or ketamine/xylazine. The potential influence of anesthesia on the signal of interest must be carefully considered (112). Examples of changes in drug-induced physiology that can be measured with imaging technologies include the following.

**Blood flow (MRI/PET):** Blood flow, blood volume, and vascular permeability can be assessed in tumors using a variety of MRI-based techniques such as dynamic contrast-enhanced MRI (DCE MRI) (113, 114), arterial spin labeling (115, 116), and iron-oxide-based contrast MRI (117). These methods have been widely used to detect response to antiangiogenic therapies in mouse cancer models (118). Tumor blood flow measurements have also been performed using clinical PET imaging of  $^{15}\text{O}[\text{H}_2\text{O}]$  (119), and

may show future widespread use in preclinical PET. Imaging of tumor perfusion and vascularity by PET and MRI is described in more detail in Chapters 4 and 5, respectively.

*Apoptosis (BLI/SPECT/PET/MRI):* Imaging of apoptosis provides a means of assessing the extent of tumor response to cytotoxic therapy. Several *in vivo* approaches have been developed utilizing BLI, MRI, PET, and SPECT (120–124). One technique using BLI makes use of tumor cells that have been transfected with a hybrid recombinant reporter consisting of luciferase linked to the estrogen receptor (ER) regulatory domain via a cleavage site for caspase-3 (DEVD) (120). The presence of ER in the hybrid reporter renders the luciferase inactive. On activation of caspase-3 during apoptosis, the DEVD site is cleaved and the luciferase becomes active, signaling the onset of apoptosis in the presence of luciferin. Other strategies for *in vivo* imaging of apoptosis are described in Chapter 16.

*Metabolism.* PET scans using [ $^{18}\text{F}$ ]FDG provide a common approach to *in vivo* assessment of energy metabolism. Since tumors generally have elevated glucose metabolism, [ $^{18}\text{F}$ ]FDG can be used to diagnose tumors as well as monitor changes in tumor metabolism in response to therapy (125). However, these types of images must be interpreted with care because elevated glucose metabolism may be associated with other physiological processes such as macrophage activity and inflammation. Methods such as MRI or MRSI can be used to quantify the levels of metabolites such as choline, lactate, and lipids using  $^1\text{H}$ -MR, and ATP and phosphocreatine using  $^{31}\text{P}$  MR (126, 127).

### 3.6 Assessment and Early Prediction of Response

Conventional imaging methods for evaluating tumor response to therapy have generally been limited to simple morphological criteria such as an apparent reduction in tumor volume (128). Determination of these endpoints can take weeks or months, hindering timely detection of failed therapies and delaying opportunities to shift to potentially more efficacious treatment. Clearly the development of highly prognostic indicators of therapeutic benefit would be a meaningful advance; FDG-PET has proven to be useful for assessing response to therapy at early time points in cancers such as lung, colorectal, cervical, and esophageal carcinomas (129–131). Assessment of response is achieved in these cases by following the relative change in FDG uptake during tumor treatment. Other PET tracers that are associated with cellular proliferation and protein synthesis have also been used to evaluate tumor response to therapy. Further discussion may be found in Chapters 4, 7, 8, and 9.

Diffusion MRI (dMRI) has been widely used in the clinic to assess acute stroke patients (132, 133), but is being increasingly used in oncology applications for the early evaluation of tumor response to therapy. It provides a measure of the apparent diffusional mobility of water in tissue. The apparent diffusion of tissue water is influenced by diffusion barriers such as cytoplasmic structures, organelles, cell membranes, and the extracellular matrix. These break down in response to treatment. Measurement of water diffusivity by dMRI yields images or maps of the apparent diffusion coefficient (ADC). Several studies of different tumor types and models have shown that ADC within the tumor is correlated with tissue cell density (134–137). When a tumor responds to therapy, an early change in ADC can be observed, often before a measurable decrease in tumor volume (138). This has been interpreted as a decrease in tumor

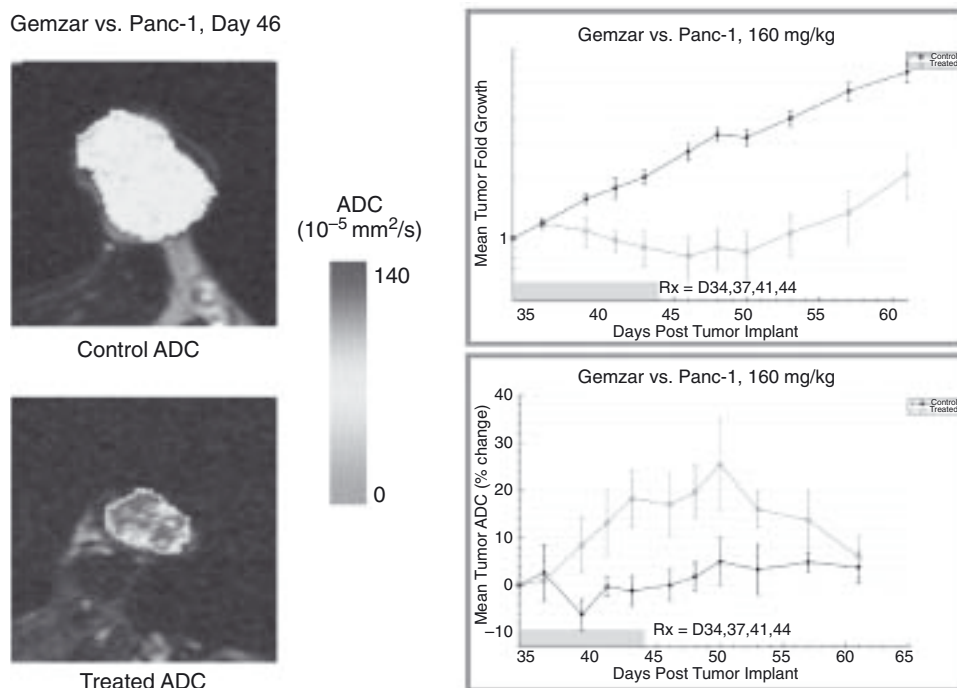


**Fig. 3.** Diffusion MRI of Panc-1 subcutaneous xenograft treated with Gemzar (160 mg/kg Q3D  $\times$  4 IP). On the left, ADC maps are shown of a single slice on day 46 for control (vehicle) and treated tumors from two different animals. Control tumor ADC values are approximately  $75 \times 10^{-5} \text{ mm}^2/\text{sec}$ ; the treated tumor has focal regions with ADC values approaching  $130 \times 10^{-5} \text{ mm}^2/\text{sec}$ . Tumor burden (mean fold growth) is plotted in the upper right panel, and mode tumor ADC change relative to pre-treatment values in the lower right panel. Open symbols are means of treated animals ( $N = 4$ ) and closed symbols are means of control animals ( $N = 4$ ).

cell density and increase in necrotic fraction (135, 136) (Fig. 3). In preclinical tumor models, this change in tumor ADC may be correlated with cell kill, providing an earlier indication of the activity of the therapeutic agent without the requisite measurement of tumor regrowth. Relative changes in ADC may also be used to optimize combination therapies or dose schedules. Recent clinical trials suggest a positive prognostic value for early ADC change in brain tumors (139). Advantages of dMRI include the following: (1) it is directly translatable to the clinic, (2) it does not require injection of contrast agents or tracers, and (3) it can be carried out with standard MRI equipment and very short scan times.

#### 4. SUMMARY AND FUTURE DIRECTIONS

A wide range of *in vivo* tumor models is available. Although most have been criticized for poor correlation with clinical outcomes, compelling evidence exists indicating that for several types of models, the absence of preclinical *in vivo* anticancer activity is a negative indicator of clinical utility (53–55). The well-recognized shift to drug discovery strategies targeting specific molecules thought to cause or support the transformed phenotype has led to increased interest in the use of orthotopic and transgenic



tumor models. These discovery strategies are also facilitated by correlation of drug effect at the molecular target with efficacy. Fortunately, recent advances in preclinical imaging technologies offer enhanced opportunities for noninvasive analysis of drug function in addition to basic tumor biology at anatomic, physiologic, and mechanistic levels. These technologies are especially well suited to the use of the increasingly relevant transgenic and orthotopic models.

With the shift toward therapeutic targeting of cancer-specific molecular defects, confirmation of the interaction of the drug with its target and analyses of downstream effects (drug-induced changes in physiology) are also frequently sought. Imaging technologies are increasingly used to this end. However, imaging at the resolution required in small animals presents many challenges. While MRI is a relatively mature modality that is now used routinely for small animal imaging, modalities such as micro-PET, micro-SPECT, and *in vivo* optical imaging have only seen widespread use in the past decade, and they pose greater challenges in terms of sensitivity and resolution. Related to these issues is the image time required, or “throughput.” Improvements in animal imaging throughput are critical in enabling meaningful and efficient animal studies that involve sufficient animal numbers and multiple time points to provide statistical power and biological relevance (140). With future technological advancements that improve sensitivity, resolution, and throughput, clinical protocols that are already used routinely in nuclear imaging, CT and MRI, will be successfully translated to true quantitative imaging in the preclinical arena. Similarly, advances in novel preclinical imaging technologies and imaging agents will be translated to clinical trial.

Quantitative imaging can offer correlations of efficacy and therapeutic index with either target modulation at the molecular level or surrogate markers of drug function. These correlations can then be used to establish decision-making thresholds for measurable endpoints in early clinical trials. Hence, the future of imaging in preclinical tumor models lies in the development and validation of image-based biomarkers and surrogate markers for tumor response that will be used in clinical trials. These technologies will be used increasingly in the earlier stages of preclinical development of new therapies as correlates for growth-based determination of efficacy.

## REFERENCES

1. Dykes D, Waud W. Murine L1210 and P388 leukemias. In: Teicher B, ed. *Tumor Models in Cancer Research*. Totowa, NJ: Humana Press, Inc., 2002:23–40.
2. Venditti JM, Humphreys SR, Goldin A. Investigation of the activity of cytoxan against leukemia L1210 in mice. *Cancer Res* 1959;19:986–995.
3. Law LW, Potter M. Further evidence of indirect induction by x-radiation of lymphocytic neoplasms in mice. *J Natl Cancer Inst* 1958;20(3):489–493.
4. Burchenal JH. Murine and human leukemias. *Bibl Haematol* 1975(40):665–677.
5. Morris HP, Slaughter LJ. Historical development of transplantable hepatomas. *Adv Exp Med Biol* 1977;92:1–19.
6. Double JA, Ball CR, Cowen PN. Transplantation of adenocarcinomas of the colon in mice. *J Natl Cancer Inst* 1975;54(1):271–275.
7. Corbett TH, Griswold DP Jr, Roberts BJ, Peckham JC, Schabel FM Jr. Biology and therapeutic response of a mouse mammary adenocarcinoma (16/C) and its potential as a model for surgical adjuvant chemotherapy. *Cancer Treat Rep* 1978;62(10):1471–1488.
8. Corbett TH, Griswold DP Jr, Roberts BJ, Peckham JC, Schabel FM Jr. Tumor induction relationships in development of transplantable cancers of the colon in mice for chemotherapy assays, with a note on carcinogen structure. *Cancer Res* 1975;35(9):2434–2439.



9. Langdon SP, Gescher A, Hickman JA, Stevens MF. The chemosensitivity of a new experimental model –the M5076 reticulum cell sarcoma. *Eur J Cancer Clin Oncol* 1984;20(5):699–705.
10. Shay H, Aegerter EA, *et al.* Development of adenocarcinoma of the breast in the Wistar rat following the gastric instillation of methylcholanthrene. *J Natl Cancer Inst* 1949;10(2):255–266.
11. Stewart HL, Hare WV, *et al.* Adenocarcinoma and other lesions of the glandular stomach of mice, following intramural injection of 20-methylcholanthrene. *J Natl Cancer Inst* 1949;10(2):359; Discussion, 99–403.
12. Fidler IJ. Selection of successive tumour lines for metastasis. *Nat New Biol* 1973;242(118):148–149.
13. Fidler IJ. Biological behavior of malignant melanoma cells correlated to their survival in vivo. *Cancer Res* 1975;35(1):218–224.
14. Morris HP. Studies on the development, biochemistry, and biology of experimental hepatomas. *Adv Cancer Res* 1965;9:227–302.
15. Skipper HE. Drug evaluation in experimental tumor systems: Potential and limitations in 1961. *Cancer Chemother Rep* 1962;16:11–18.
16. Skipper HE, Schmidt LH. A manual on quantitative drug evaluation in experimental tumor systems. I. Background, description of criteria, and presentation of quantitative therapeutic data on various classes of drugs obtained in diverse experimental tumor systems. *Cancer Chemother Rep* 1962;17:1–143.
17. Skipper HE. Cancer chemotherapy is many things: G.H.A. Clowes Memorial Lecture. *Cancer Res* 1971;31(9):1173–1180.
18. Schabel FM Jr. Screening, the cornerstone of chemotherapy. *Cancer Chemother Rep* 2 1972;3(1):309–313.
19. Schabel FM Jr, Corbett TH. Cell kinetics and the chemotherapy of murine solid tumors. *Antibiot Chemother* 1980;28:28–34.
20. Schabel FM Jr, Montgomery JA, Skipper HE, Laster WR Jr, Thomson JR. Experimental evaluation of potential anticancer agents. I. Quantitative therapeutic evaluation of certain purine analogs. *Cancer Res* 1961;21:690–699.
21. Griswold DP Jr, Casey AE, Weisburger EK, Weisburger JH, Schabel FM Jr. On the carcinogenicity of a single intragastric dose of hydrocarbons, nitrosamines, aromatic amines, dyes, coumarins, and miscellaneous chemicals in female Sprague-Dawley rats. *Cancer Res* 1966;26(4):619–625.
22. Griswold DP, Corbett TH. A colon tumor model for anticancer agent evaluation. *Cancer* 1975;36(6 Suppl):2441–2444.
23. Griswold DP, Skipper HE, Laster WR Jr, Wilcox WS, Schabel FM Jr. Induced mammary carcinoma in the female rat as a drug evaluation system. *Cancer Res* 1966;26(10):2169–2180.
24. Corbett TH, Roberts BJ, Leopold WR, *et al.* Induction and chemotherapeutic response of two transplantable ductal adenocarcinomas of the pancreas in C57BL/6 mice. *Cancer Res* 1984;44(2):717–726.
25. Roberts BJ, Fife WP, Corbett TH, Schabel FM. Response of five established solid transplantable mouse tumors and one mouse leukemia to hyperbaric hydrogen. *Cancer Treat Rep* 1978;62(7):1077–1079.
26. Tapazoglou E, Polin L, Corbett TH, al-Sarraf M. Chemotherapy of the squamous cell lung cancer LC-12 with 5-fluorouracil, cisplatin, carboplatin or iproplatin combinations. *Invest New Drugs* 1988;6(4):259–264.
27. Schabel FM, Griswold DP, Laster WR, Corbett TH, Lloyd HH. Quantitative evaluation of anticancer agent activity in experimental animals. *Pharmacol Ther Part A: Chemother Toxicol Metabol Inhibit* 1977;1(4):411–435.
28. Venditti JM, Wesley RA, Plowman J. Current NCI preclinical antitumor screening in vivo: Results of tumor panel screening, 1976–1982, and future directions. *Adv Pharmacol Chemother* 1984;20:1–20.
29. Zee-Cheng RK, Cheng CC. Screening and evaluation of anticancer agents. *Methods Find Exp Clin Pharmacol* 1988;10(2):67–101.
30. Jackson RC. The problem of the quiescent cancer cell. *Adv Enzyme Regul* 1989;29:27–46.
31. DiGiovanni J. Modification of multistage skin carcinogenesis in mice. *Prog Exp Tumor Res* 1991;33:192–229.
32. Konishi Y, Tsutsumi M, Tsujiuchi T. Mechanistic analysis of pancreatic ductal carcinogenesis in hamsters. *Pancreas* 1998;16(3):300–306.

33. Miller MS, Leone-Kabler S, Rollins LA, *et al.* Molecular pathogenesis of transplacentally induced mouse lung tumors. *Exp Lung Res* 1998;24(4):557–577.
34. Russo J, Russo IH. Experimentally induced mammary tumors in rats. *Breast Cancer Res Treat* 1996;39(1):7–20.
35. Nakagama H, Ochiai M, Ubagai T, *et al.* A rat colon cancer model induced by 2-amino-1-methyl-6-phenylimidazo[4,5-b]pyridine, PhIP. *Mutat Res* 2002;506–507:137–144.
36. Aamdal S, Fodstad O, Pihl A. Human tumor xenografts transplanted under the renal capsule of conventional mice. Growth rates and host immune response. *Int J Cancer* 1984;34(5):725–730.
37. Bogden AE. The subrenal capsule assay (SRCA) and its predictive value in oncology. *Ann Chir Gynaecol Suppl* 1985;199:12–27.
38. Simmons ML, Richter CB, Tennant RW, Franklin J. Production of specific pathogen-free rats in plastic germfree isolator rooms. In: Symposium on Gnotobiotic Life in Medical and Biological Research, 1968.
39. (U.S.) IoLAR, NetLibrary I. Guide for the care and use of laboratory animals. National Research Council, 1996.
40. Custer RP, Bosma GC, Bosma MJ. Severe combined immunodeficiency (SCID) in the mouse. Pathology, reconstitution, neoplasms. *Am J Pathol* 1985;120(3):464–477.
41. Dorshkind K, Keller GM, Phillips RA, *et al.* Functional status of cells from lymphoid and myeloid tissues in mice with severe combined immunodeficiency disease. *J Immunol* 1984;132(4):1804–1808.
42. Eaton GJ. Hair growth cycles and wave patterns in “nude” mice. *Transplantation* 1976;22(3):217–222.
43. Flanagan SP. “Nude”, a new hairless gene with pleiotropic effects in the mouse. *Genet Res* 1966;8(3):295–309.
44. Bosma GC, Custer RP, Bosma MJ. A severe combined immunodeficiency mutation in the mouse. *Nature* 1983;301(5900):527–530.
45. Bosma GC, Davisson MT, Ruetsch NR, Sweet HO, Shultz LD, Bosma MJ. The mouse mutation severe combined immune deficiency (scid) is on chromosome 16. *Immunogenetics* 1989;29(1):54–57.
46. Clark EA, Shultz LD, Pollack SB. Mutations in mice that influence natural killer (NK) cell activity. *Immunogenetics* 1981;12(5–6):601–613.
47. Mahoney KH, Morse SS, Morahan PS. Macrophage functions in beige (Chediak-Higashi syndrome) mice. *Cancer Res* 1980;40(11):3934–3939.
48. Roder J, Duwe A. The beige mutation in the mouse selectively impairs natural killer cell function. *Nature* 1979;278(5703):451–453.
49. Saxena RK, Saxena QB, Adler WH. Defective T-cell response in beige mutant mice. *Nature* 1982;295(5846):240–241.
50. Scher I, Frantz MM, Steinberg AD. The genetics of the immune response to a synthetic double-stranded RNA in a mutant CBA mouse strain. *J Immunol* 1973;110(5):1396–1401.
51. Kerbel RS. Human tumor xenografts as predictive preclinical models for anticancer drug activity in humans: Better than commonly perceived—but they can be improved. *Cancer Biol Ther* 2003;2(4 Suppl 1):S134–139.
52. Suggitt M, Bibby MC. 50 years of preclinical anticancer drug screening: Empirical to target-driven approaches. *Clin Cancer Res* 2005;11(3):971–981.
53. Voskoglou-Nomikos T, Pater JL, Seymour L. Clinical predictive value of the in vitro cell line, human xenograft, and mouse allograft preclinical cancer models. *Clin Cancer Res* 2003;9(11):4227–4239.
54. Jackson RC, Sebolt JS, Shillis JL, Leopold WR. The pyrazoloacridines: Approaches to the development of a carcinoma-selective cytotoxic agent. *Cancer Invest* 1990;8(1):39–47.
55. Johnson JI, Decker S, Zaharevitz D, *et al.* Relationships between drug activity in NCI preclinical in vitro and in vivo models and early clinical trials. *Br J Cancer* 2001;84(10):1424–1431.
56. Decker S, Hollingshead M, Bonomi CA, Carter JP, Sausville EA. The hollow fibre model in cancer drug screening: The NCI experience. *Eur J Cancer* 2004;40(6):821–826.
57. Hall LA, Krauthauser CM, Wexler RS, Slee AM, Kerr JS. The hollow fiber assay. *Methods Mol Med* 2003;74:545–566.

58. Fidler IJ, Wilmanns C, Staroselsky A, Radinsky R, Dong Z, Fan D. Modulation of tumor cell response to chemotherapy by the organ environment. *Cancer Metastasis Rev* 1994;13(2):209–222.
59. Killion JJ, Radinsky R, Fidler IJ. Orthotopic models are necessary to predict therapy of transplantable tumors in mice. *Cancer Metastasis Rev* 1998;17(3):279–284.
60. Singh RK, Tsan R, Radinsky R. Influence of the host microenvironment on the clonal selection of human colon carcinoma cells during primary tumor growth and metastasis. *Clin Exp Metastasis* 1997;15(2):14–50.
61. Hart IR. “Seed and soil” revisited: Mechanisms of site-specific metastasis. *Cancer Metastasis Rev* 1982;1(1):5–16.
62. Fidler IJ. The pathogenesis of cancer metastasis: The “seed and soil” hypothesis revisited. *Nat Rev Cancer* 2003;3(6):453–458.
63. Paget S. The distribution of secondary growths in cancer of the breast. *Lancet* 1889;1:571–573.
64. Radinsky R. Modulation of tumor cell gene expression and phenotype by the organ-specific metastatic environment. *Cancer Metastasis Rev* 1995;14(4):3–38.
65. Clarke AR, Hollstein M. Mouse models with modified p53 sequences to study cancer and ageing. *Cell Death Differ* 2003;10(4):44–50.
66. Kavanaugh CJ, Desai KV, Calvo A, *et al.* Pre-clinical applications of transgenic mouse mammary cancer models. *Transgenic Res* 2002;11(6):61–133.
67. Kwak I, Tsai SY, DeMayo FJ. Genetically engineered mouse models for lung cancer. *Annu Rev Physiol* 2004;66:647–663.
68. Lakhtakia R, Panda SK. Transgenic mouse models and hepatocellular carcinoma: Future prospects. *Trop Gastroenterol* 2000;21(3):91–94.
69. Lowy AM. Transgenic models of pancreatic cancer. *Int J Gastrointest Cancer* 2003;33(1):71–78.
70. Lubet RA, Zhang Z, Wiseman RW, You M. Use of p53 transgenic mice in the development of cancer models for multiple purposes. *Exp Lung Res* 2000;26(8):58–93.
71. Kasper S, Smith JA Jr. Genetically modified mice and their use in developing therapeutic strategies for prostate cancer. *J Urol* 2004;172(1):12–19.
72. Gingrich JR, Barrios RJ, Morton RA, *et al.* Metastatic prostate cancer in a transgenic mouse. *Cancer Res* 1996;56(18):4096–4102.
73. Macleod KF, Jacks T. Insights into cancer from transgenic mouse models. *J Pathol* 1999;187(1):43–60.
74. Deng CX, Brodie SG. Knockout mouse models and mammary tumorigenesis. *Semin Cancer Biol* 2001;11(5):38–94.
75. Fisher GH, Orsulic S, Holland EC, *et al.* Development of a flexible and specific gene delivery system from production of murine tumor models. *Oncogene* 1999;18:5253–5260.
76. McConville P, Hambardzumyan D, Moody JB, Leopold WR, Kreger AR, Woolliscroft MJ, Rehemtulla A, Ross BD, Holland EC. MRI determination of tumor grade and early response to temozolomide in a genetically engineered mouse model of glioma. *Clin Cancer Res* 2007, in press.
77. Orsulic S. An RCAS-tva-based approach to designer mouse models. *Mammalian Genome* 2002;13:543–547.
78. Orsulic S, Li Y, Soslow RA, Vitale-Cross LA, Gutkind JS, Varmus HE. Induction of ovarian cancer by defined multiple genetic changes in a mouse model. *Cancer Cell* 2002;1:53–62.
79. Contag CH. Bioluminescence imaging of mouse models of human cancer. In: Holland EC, ed. *Mouse Models of Human Cancer*. Hoboken, NJ: John Wiley & Sons, Inc., 2004:363–373.
80. Edinger M, Cao YA, Hornig YS, *et al.* Advancing animal models of neoplasia through in vivo bioluminescence imaging. *Eur J Cancer* 2002;38(16):2128–2136.
81. Choy G, Choyke P, Libutti SK. Current advances in molecular imaging: Noninvasive in vivo bioluminescent and fluorescent optical imaging in cancer research. *Mol Imaging* 2003;2(4):303–312.
82. Choy G, O’Connor S, Diehn FE, *et al.* Comparison of noninvasive fluorescent and bioluminescent small animal optical imaging. *Biotechniques* 2003;35(5):1022–1026.
83. Contag CH, Bachmann MH. Advances in in vivo bioluminescence imaging of gene expression. *Annu Rev Biomed Eng* 2002;4:235–260.
84. Jaffer FA, Weissleder R. Molecular imaging in the clinical arena. *JAMA* 2005;293(7):855–862.
85. Benaron DA. The future of cancer imaging. *Cancer Metastasis Rev* 2002;21(1):45–78.

86. Muruganandham M, Koutcher JA. Magnetic resonance imaging in mouse cancer models. In: Holland EC, ed. *Micro-Computed Tomography of Mouse Cancer Models*. Hoboken, NJ: John Wiley & Sons, Inc., 2004:349–362.
87. Pautler RG. Mouse MRI: Concepts and applications in physiology. *Physiology (Bethesda)* 2004; 19:168–175.
88. Swindle P, McCredie S, Russell P, et al. Pathologic characterization of human prostate tissue with proton MR spectroscopy. *Radiology* 2003;228(1):144–151.
89. Weichert JP. Micro-computed tomography of mouse cancer models. In: Holland EC, ed. *Mouse Models of Human Cancer*. Hoboken, NJ: John Wiley & Sons, Inc., 2004:339–348.
90. Spence AM, Mankoff DA, Muzi M. Positron emission tomography imaging of brain tumors. *Neuroimaging Clin North Am* 2003;13(4):717–739.
91. Shields AF, Grierson JR, Dohmen BM, et al. Imaging proliferation in vivo with [F-18]FLT and positron emission tomography. *Nat Med* 1998;4(11):1334–1336.
92. Shields AF, Mankoff DA, Link JM, et al. Carbon-11-thymidine and FDG to measure therapy response. *J Nucl Med* 1998;39(10):1757–1762.
93. Jager PL, Que TH, Vaalburg W, Pruim J, Elsinga P, Plukker JT. Carbon-11 choline or FDG-PET for staging of oesophageal cancer? *Eur J Nucl Med* 2001;28(12):184–189.
94. Jager PL, Vaalburg W, Pruim J, de Vries EG, Langen KJ, Piers DA. Radiolabeled amino acids: Basic aspects and clinical applications in oncology. *J Nucl Med* 2001;42(3):432–445.
95. Furumoto S, Takashima K, Kubota K, Ido T, Iwata R, Fukuda H. Tumor detection using 18F-labeled matrix metalloproteinase-2 inhibitor. *Nucl Med Biol* 2003;30(2):119–125.
96. Gambhir S, Herschman H, Cherry S, et al. Imaging transgene expression with radionuclide imaging technologies. *Neoplasia* 2000;2(1–2):118–138.
97. Lee FT, Hall C, Rigopoulos A, et al. Immuno-PET of human colon xenograft-bearing BALB/c nude mice using 124I-CDR-grafted humanized A33 monoclonal antibody. *J Nucl Med* 2001;42(5):764–769.
98. Sundaresan G, Yazaki PJ, Shively JE, et al. 124I-labeled engineered anti-CEA minibodies and diabodies allow high-contrast, antigen-specific small-animal PET imaging of xenografts in athymic mice. *J Nucl Med* 2003;44(12):1962–1969.
99. Rockwell S. Tumor cell survival. In: Teicher B, ed. *Tumor Models in Cancer Research*. Totowa, NJ: Humana Press, Inc., 2002:617–631.
100. Dykes DJ, Abbott BJ, Mayo JG, et al. Development of human tumor xenograft models for in vivo evaluation of new antitumor drugs. *Contrib Oncol* 1992;42:1–22.
101. Plowman J. Human tumor xenograft models in NCI drug development. In: Teicher B, ed. *Anticancer Drug Development Guide: Preclinical Screening, Clinical Trials, and Approval*. Totowa, NJ: Humana Press, 1997:10–25.
102. Coe RA. Quantitative whole-body autoradiography. *Regul Toxicol Pharmacol* 2000;31(2 Pt 2):S1–3.
103. Malandain G, Bardin E, Nelissen K, Vanduffel W. Fusion of autoradiographs with an MR volume using 2-D and 3-D linear transformations. *Neuroimage* 2004;23(1):111–27.
104. Fischman AJ, Alpert NM, Rubin RH. Pharmacokinetic imaging: A noninvasive method for determining drug distribution and action. *Clin Pharmacokinet* 2002;41(8):581–602.
105. Sebolt-Leopold JS, Dudley DT, Herrera R, et al. Blockade of the MAP kinase pathway suppresses growth of colon tumors in vivo. *Nat Med* 1999;5(7):810–816.
106. Mendel DB, Laird AD, Xin X, et al. In vivo antitumor activity of SU11248, a novel tyrosine kinase inhibitor targeting vascular endothelial growth factor and platelet-derived growth factor receptors: Determination of a pharmacokinetic/pharmacodynamic relationship. *Clin Cancer Res* 2003;9(1):327–337.
107. Fry DW, Harvey PJ, Keller PR, et al. Specific inhibition of cyclin-dependent kinase 4/6 by PD 0332991 and associated antitumor activity in human tumor xenografts. *Mol Cancer Ther* 2004; 3(11):1427–1438.
108. Ross BD, Chenevert TL, Moffat BA, et al. Use of magnetic resonance imaging for evaluation of treatment response. In: Holland EC, ed. *Mouse Models of Human Cancer*. Hoboken, NJ: John Wiley & Sons, Inc., 2004:377–390.
109. Willett CG, Boucher Y, di Tomaso E, et al. Direct evidence that the VEGF-specific antibody bevacizumab has antivasculature effects in human rectal cancer. *Nat Med* 2004;10(2):145–147.
110. Galbraith SM, Maxwell RJ, Lodge MA, et al. Combretastatin A4 phosphate has tumor antivasculature activity in rat and man as demonstrated by dynamic magnetic resonance imaging. *J Clin Oncol* 2003;21(15):2831–2842.

111. Galbraith SM. Antivascular cancer treatments: Imaging biomarkers in pharmaceutical drug development. *Br J Radiol* 2003;76(Spec No 1):S83–S86.
112. Toyama H, Ichise M, Liow JS, *et al.* Evaluation of anesthesia effects on [18F]FDG uptake in mouse brain and heart using small animal PET. *Nucl Med Biol* 2004;31(2):251–256.
113. Taylor JS, Tofts PS, Port R, *et al.* MR imaging of tumor microcirculation: Promise for the new millennium. *J Magn Reson Imaging* 1999;10(6):90–97.
114. Leach MO, Brindle KM, Evelhoch JL, *et al.* Assessment of antiangiogenic and antivascular therapeutics using MRI: Recommendations for appropriate methodology for clinical trials. *Br J Radiol* 2003;76(Spec No 1):S87–S91.
115. Moffat BA, Chenevert TL, Hall DE, Rehemtulla A, Ross BD. Continuous arterial spin labeling using a train of adiabatic inversion pulses. *J Magn Reson Imaging* 2005;21(3):290–296.
116. Sun Y, Schmidt NO, Schmidt K, *et al.* Perfusion MRI of U87 brain tumors in a mouse model. *Magn Reson Med* 2004;51(5):893–899.
117. Moffat BA, Reddy GR, McConville P, *et al.* A novel polyacrylamide magnetic nanoparticle contrast agent for molecular imaging using MRI. *Mol Imaging* 2003;2(4):324–332.
118. Miller JC, Pien HH, Sahani D, Sorensen AG, Thrall JH. Imaging angiogenesis: Applications and potential for drug development. *J Natl Cancer Inst* 2005;97(3):172–187.
119. Anderson H, Price P. Clinical measurement of blood flow in tumours using positron emission tomography: A review. [Article]. *Nucl Med Commun* 2002;23(2):131–138.
120. Laxman B, Hall DE, Bhojani MS, *et al.* Noninvasive real-time imaging of apoptosis. *Proc Natl Acad Sci USA* 2002;99(26):16551–16555.
121. Jung HI, Kettunen MI, Davletov B, Brindle KM. Detection of apoptosis using the C2A domain of synaptotagmin I. *Bioconjug Chem* 2004;15(5):983–987.
122. Hakumaki JM, Brindle KM. Techniques: Visualizing apoptosis using nuclear magnetic resonance. *Trends Pharmacol Sci* 2003;24(3):146–149.
123. Collingridge DR, Glaser M, Osman S, *et al.* In vitro selectivity, in vivo biodistribution and tumour uptake of annexin V radiolabelled with a positron emitting radioisotope. *Br J Cancer* 2003;89(7):1327–1333.
124. Zhao M, Beauregard DA, Loizou L, Davletov B, Brindle KM. Non-invasive detection of apoptosis using magnetic resonance imaging and a targeted contrast agent. *Nat Med* 2001;7(11):1241–1244.
125. Phelps ME. Inaugural article: Positron emission tomography provides molecular imaging of biological processes. *Proc Natl Acad Sci USA* 2000;97(16):9226–9233.
126. Maxwell RJ, Nielsen FU, Breidahl T, Stodkilde-Jorgensen H, Horsman MR. Effects of combretastatin on murine tumours monitored by 31P MRS, 1H MRS and 1H MRI. *Int J Radiat Oncol Biol Phys* 1998;42(4):891–894.
127. Kristensen CA, Askenasy N, Jain RK, Koretsky AP. Creatine and cyclocreatine treatment of human colon adenocarcinoma xenografts: 31P and 1H magnetic resonance spectroscopic studies. *Br J Cancer* 1999;79(2):278–285.
128. Therasse P, Arbuck SG, Eisenhauer EA, *et al.* New guidelines to evaluate the response to treatment in solid tumors. European Organization for Research and Treatment of Cancer, National Cancer Institute of the United States, National Cancer Institute of Canada. *J Natl Cancer Inst* 2000;92(3):205–216.
129. Stahl A, Ott K, Schwaiger M, Weber WA. Comparison of different SUV-based methods for monitoring cytotoxic therapy with FDG PET. *Eur J Nucl Med Mol Imaging* 2004;31(11):1471–1478.
130. Stahl A, Wieder H, Piert M, Wester HJ, Senekowitsch-Schmidtke R, Schwaiger M. Positron emission tomography as a tool for translational research in oncology. *Mol Imaging Biol* 2004;6(4):214–224.
131. Stahl A, Wieder H, Wester HJ, *et al.* PET/CT molecular imaging in abdominal oncology. *Abdom Imaging* 2004;29(3):388–397.
132. Xavier AR, Qureshi AI, Kirmani JF, Yahia AM, Bakshi R. Neuroimaging of stroke: A review. *South Med J* 2003;96(4):367–379.
133. Roberts TP, Rowley HA. Diffusion weighted magnetic resonance imaging in stroke. *Eur J Radiol* 2003;45(3):185–194.
134. Chenevert TL, Stegman LD, Taylor JMG, *et al.* Diffusion magnetic resonance imaging: An early surrogate marker of therapeutic efficacy in brain tumors. *J Natl Cancer Inst* 2000;92(24):2029–2036.

135. Chenevert TL, McKeever PE, Ross BD. Monitoring early response of experimental brain tumors to therapy using diffusion magnetic resonance imaging. *Clin Cancer Res* 1997;3(9):1457–1466.
136. Lyng H, Haraldseth O, Rofstad EK. Measurement of cell density and necrotic fraction in human melanoma xenografts by diffusion weighted magnetic resonance imaging. *Magn Reson Med* 2000;43(6):828–836.
137. Sugahara T, Korogi Y, Kochi M, *et al.* Usefulness of diffusion-weighted MRI with echo-planar technique in the evaluation of cellularity in gliomas. *J Magn Reson Imaging* 1999;9(1):53–60.
138. Ross BD, Moffat BA, Lawrence TS, *et al.* Evaluation of cancer therapy using diffusion magnetic resonance imaging. *Mol Cancer Ther* 2003;2(6):581–587.
139. Moffat BA, Chenevert TL, Lawrence T, *et al.* Functional diffusion map: A noninvasive MRI biomarker for early stratification of clinical brain tumor response. *Proc Natl Acad Sci USA* 2005; 102(15):5524–5529.
140. McConville P, Moody JB, Moffat BA. High-throughput magnetic resonance imaging in mice for phenotyping and therapeutic evaluation. *Curr Opin Chem Biol* 2005;9(4):413–420.



In Vivo Imaging of Cancer Therapy

Shields, A.F.; Price, P. (Eds.)

2007, XII, 326 p., Hardcover

ISBN: 978-1-58829-633-7

A product of Humana Press